

Catalytic Ozonation by Chalcopyrite for the Degradation of Oxalic Acid in Water

Bokang Liu¹, Xiaoyue Wang², Siru Zhang³ and Junkai Zhao⁴

Bokang Liu: Email: 549095488@qq.com, School of Environment and Architecture, University of Shanghai for Science and Technology, Shanghai, P.R. China, 200093

Xiaoyue Wang: Email: 1551258429@qq.com, School of Environment and Architecture, University of Shanghai for Science and Technology, Shanghai, P.R. China, 200093

Siru Zhang: Email: 1063794912@qq.com, School of Environment and Architecture, University of Shanghai for Science and Technology, Shanghai, P.R. China, 200093

Junkai Zhao: Email: 1392652017@qq.com, School of Environment and Architecture, University of Shanghai for Science and Technology, Shanghai, P.R. China, 200093

Corresponding Author: Bokang Liu

Abstract

Natural chalcopyrite was ground into powder and used for ozonation to degrade oxalic acid in water. The effects of initial pH, chalcopyrite dosage, ozone dosage and initial concentration of oxalic acid on the removal of oxalic acid by heterogeneous ozonation were investigated and the chalcopyrite was characterized by FTIR (Fourier transform infrared spectroscopy), SEM (Scanning electron microscope) and XPS (X-ray photoelectron spectroscopy). The experimental results show that under the optimum conditions, the removal of oxalic acid could reach 91.3%. The surface of chalcopyrite is rich in surface hydroxyl groups. From free radical quenching experiments it was found that there might be more than one Reactive oxygen Species (ROS) in chalcopyrite / O₃ system. The possible mechanism of oxalic acid degradation by chalcopyrite catalyzed ozonation was proposed.

Keywords: Catalytic ozonation; Chalcopyrite; Oxalic acid

Date of Submission: 10-03-2023

Date of acceptance: 23-03-2023

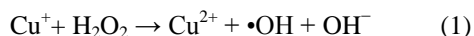
I. INTRODUCTION

Advanced oxidation processes (AOPs), such as Fenton, ozonation, photocatalysis, have been extensively applied in water and wastewater treatment, especially for the degradation of persistent and toxic organic pollutants^{[32][12]}. In the field of environmental remediation, researchers have used AOPS as a powerful tool for generating of ROS to degrade persistent and recalcitrant organic pollutants into harmless small molecules such as carbon dioxide (CO₂), mineralized salts and water (H₂O)^[1].

Ozone is an unstable gas with a characteristic penetrating odor and is partially soluble in water. Ozone is also a powerful oxidant with a REDOX potential of 2.07V in alkaline solutions^[23]. Therefore, ozone is able to oxidize a large number of inorganic and organic materials. However, the instability and reaction selectivity of ozone make it less efficient in degrading pollutants, which has led to a series of technologies combined with ozone, such as hydrogen peroxide, ultraviolet radiation, ultrasound, etc^[24]. The process of combining ozonation with other chemicals or processes to improve the generation of hydroxyl radicals during ozonation to achieve homogeneous or heterogeneous catalytic ozonation, have become research hotspot. Due to the introduction of transition metal ion catalysts, homogeneous catalytic ozonation suffers from difficulties in catalyst recovery and secondary pollution. In contrast, heterogeneous catalytic ozonation with solid catalysts shows a broad application prospect in wastewater treatment^[21].

Oxalic acid (OA) is one of the most commonly ozonation inter-mediate of carboxylic acids and the main component of residual total organic carbon, which has a very slow reaction rate with O₃ (k_{O₃}=0.04 M⁻¹·s⁻¹)^{[28][26]}, and high reactivity (k ≈ 106 M⁻¹·s⁻¹) towards hydroxyl radicals (•OH) generated from the decomposition of ozone in aqueous solution.^{[9][4]} Therefore, oxalic acid was selected as the target organic chemicals to make imulated waste water.

Chalcopyrite (CuFeS₂) is the most abundant copper mineral among all kinds of copper sulfide ores^[25]. Also, Chalcopyrite (CuFeS₂) is an iron sulfide mineral containing copper ions that can enhance the degradation process by producing more •OH from the Fenton-like reaction (Eq. (1))^[21].



Another study expected that chalcopyrite represents a promising alternative Fenton catalyst attributed to the immediate release of Fe^{2+} , Cu^{2+} , and protons.^{[8][16][11]} The same advanced oxidation process also uses reactive oxygen species such as hydroxyl radicals generated in the reaction system to degrade organic pollutants. Therefore, chalcopyrite was used as catalyst to investigate the effects of different factors on oxalic acid removal in the process of catalytic ozonation, and the possible mechanism of chalcopyrite catalyzed ozonation was discussed.

II. MATERIALS AND METHODS

Reagents and materials

Oxalic acid dihydrate ($\text{C}_2\text{H}_2\text{O}_4 \cdot 2\text{H}_2\text{O}$), sodium hydroxide (NaOH), hydrochloric acid (HCl) and anhydrous dipotassium hydrogen phosphate (K_2HPO_4), sodium bicarbonate (NaHCO_3) were purchased from Sinopharm Chemical Reagent (Shanghai), all of which were of analytical grade, and all solutions were prepared with deionized water.

Natural chalcopyrite (NCP) raw ore was obtained from Daye City, Hubei Province, China. The sample was crushed until it could pass through a 325 mesh sieve to obtain fine particles. The NCP was not pretreated in any other way to better evaluate the natural minerals.

Catalytic ozonation

This experiment was carried out at room temperature (20°C - 25°C) in a glass reactor (volume of 1 L). First, a solution of oxalic acid with a Total Organic Carbon (TOC) concentration of 10 mg/L was added to the reaction vessel, and the initial pH of the solution was adjusted using sodium hydroxide or hydrochloric acid and measured with a pH meter (PXSJ-226, Shanghai INESA Company). A certain amount of chalcopyrite was added to the oxalic acid solution. At the same time, the ozone generator (KX-S10/OY-3L, Shanghai Kangxiao Environmental Protection Co., Ltd.) was turned on so that a certain flow rate of ozone gas was blown into the solution through a sintered glass diffuser. The flow rate is measured out by a mass flow meter (2SLM-B01, Shanghai Kangxiao Environmental Protection Co., Ltd.). A glass syringe was used during the reaction to take samples from the sampling port at different times, after the sample was purged with nitrogen to blow off the ozone, then filtered through a $0.45 \mu\text{m}$ filter membrane for TOC (MULTERN/C3100 TOC tester, Jena, Germany) determination

Characterization Techniques

The infrared spectra of natural chalcopyrite and chalcopyrite after catalytic ozonation in the range of 4000 - 500 cm^{-1} were obtained by Fourier transform infrared spectroscopy (FTIR, Tensor 27 Germany). The valence states of Fe, Cu, S, O and C in the catalyst were determined by X-ray photoelectron spectroscopy (XPS, Thermo Fischer, Escalab Xi+). The microstructure of chalcopyrite was observed by scanning electron microscope (SEM, Zeiss, GEMINI300).

III. Results and discussion

Characteristics of chalcopyrite

1. FT-IR

Figure 1 shows the FT-IR spectral characterization of chalcopyrite from 500 to 4000 cm^{-1} . By comparing the spectra before and after ozonation, the characteristic vibrational peaks of chalcopyrite can be seen: 3409 cm^{-1} and 1631 cm^{-1} can be attributed to the -OH stretching vibration of chalcopyrite surface and the H-OH bending vibration of crystalline water, respectively. The peak at 1397 cm^{-1} is attributed to the adsorbed CO_2 or the C=O stretching vibration of oxalic acid left on the surface of chalcopyrite^[11]. The absorption peaks at 1099 cm^{-1} and 749 cm^{-1} can be attributed to the Fe-S stretching vibration; 1047 cm^{-1} can be attributed to the S-O vibration of sulfur compounds, which may be caused by the oxidation of S^{2-} to SO_4^{2-} and other sulfate-like substances after the reaction. The absorption peak at 578 cm^{-1} represents the Fe-O group^[20]. A small area near 508 cm^{-1} has a stretching vibration peak corresponding to Cu-S^[7]. Therefore, after catalytic ozonation, some of the vibration peaks of chalcopyrite changed obviously and there were oxides formed on its surface, which is consistent with the characterization results of XPS.

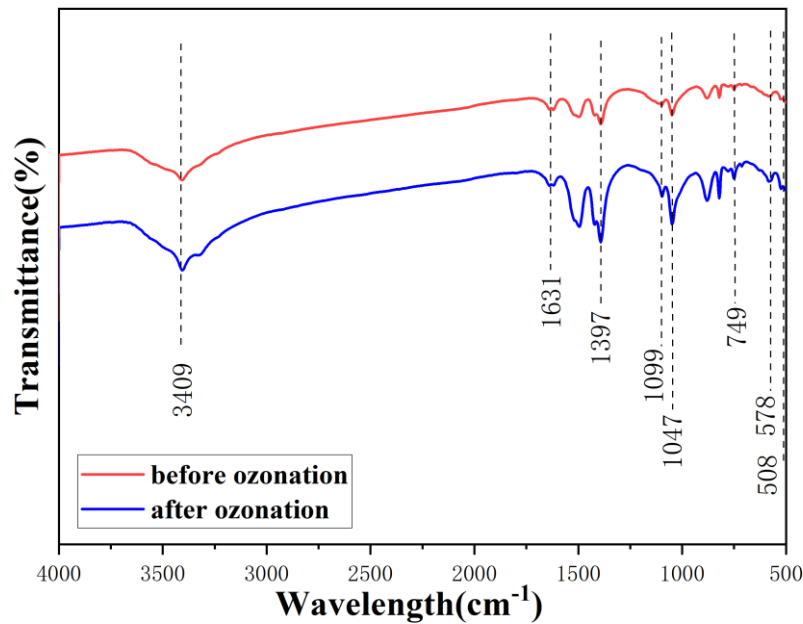


Fig. 1 FT-IR of chalcopyrite before and after reaction

2. XPS

The composition, chemical valence, surface electron distribution and energy level structure of chemical elements on the surface of chalcopyrite were analyzed by XPS.

Fig.2 indicates that there are mainly Cu 2p, Fe 2p, O 1s, C 1s and S 2p orbital peaks in the chalcopyrite XPS spectra before and after ozonation, so the main elements are S, O, C, Fe and Cu. The C element is speculated to be the adsorption of pollutants or impurities on the material surface.

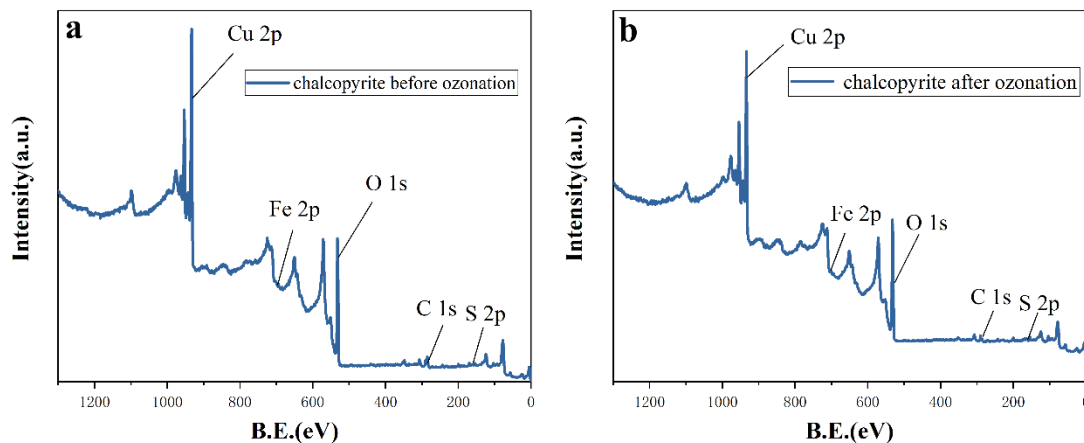


Fig. 2 XPS spectra of chalcopyrite (a) before and (b) after ozonation

2.1 Fe 2p and Cu 2p before and after ozonation

In Fig.3 (a), Cu 2p_{3/2} and Cu2p_{1/2} appear at binding energies of 933.2 eV and 952.9 eV, and the inverse convolution of the Cu 2p_{3/2} region is two peaks, indicating that the same major valence states of Cu⁺¹ 933.0 eV and Cu²⁺ 934.1 eV on the surface of fresh chalcopyrite and chalcopyrite after ozonation. Similarly, as observed in Fig.3 (b), the peaks at binding energies 712.5 eV, 724.5 eV attributed to Fe 2p_{3/2} and Fe 2p_{1/2}, respectively, were fitted to four peaks in the deconvoluted Fe 2p spectrum. Peaks near 710.9 eV and 723.7 eV can be attributed to Fe²⁺, while the peaks at 713.8 eV and 726.0 eV were attributed to Fe³⁺[18].

The proportion of Cu^{+1} after ozonation decreased from 48.22% to 41.28%, while Cu^{2+} increased from 51.60% to 58.60%. The ratio of Fe^{3+} to Fe^{2+} changed from 1.18 to 1.50, indicating that some metal oxides were formed on the surface of chalcopyrite after ozonation. The results also show that hydroxyl groups are more easily adsorbed on the Fe site, and the surface hydroxylation of Fe site is more spontaneous than that of Cu site. So Fe is more likely to be oxidized by O_3 or $\cdot\text{OH}$ than Cu [29].

Studies have shown that sulfur substances (S^{2-} , S_2^{2-} and S_n^{2-}) played a key role in promoting the cycle of $\text{Cu}^{2+}/\text{Cu}^{+}$ and $\text{Fe}^{3+}/\text{Fe}^{2+}$ in chalcopyrite / O_3 system, resulting in a change in the proportion of the four sulfur species (Eq. (2)-(8)) [22], it is speculated that the following reactions might exist in the chalcopyrite/ O_3 system.

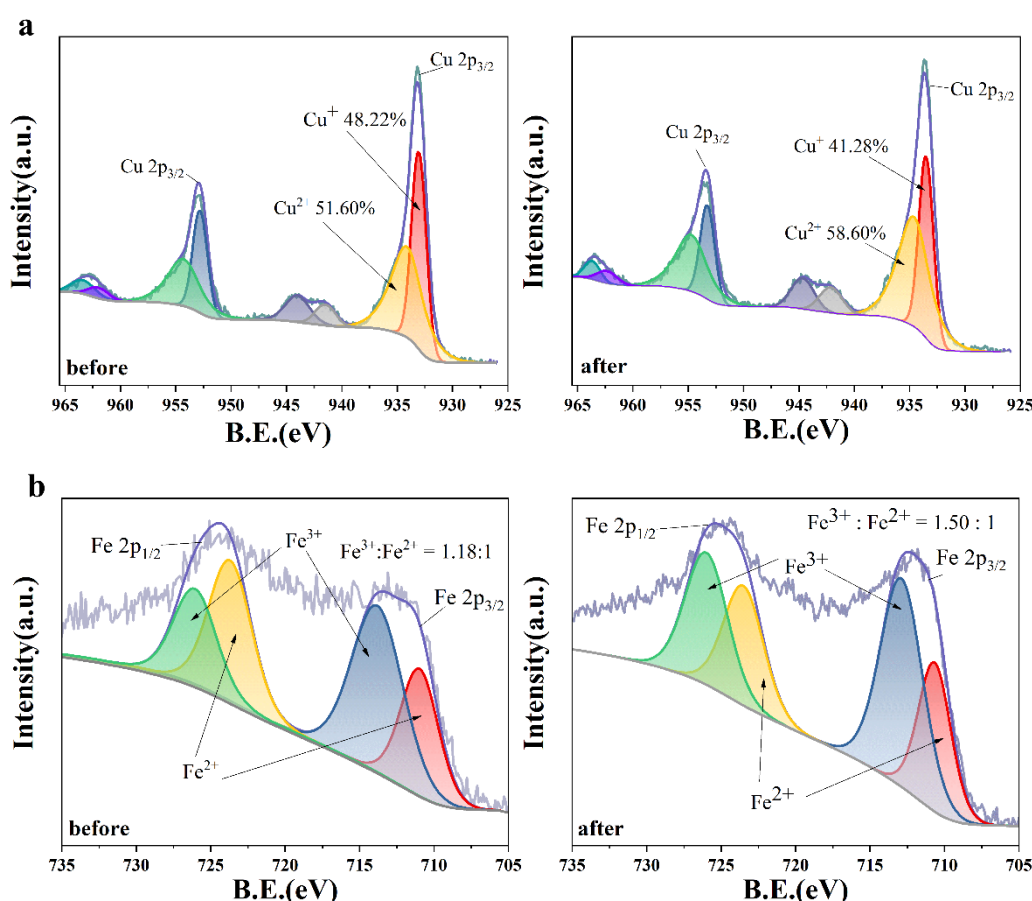
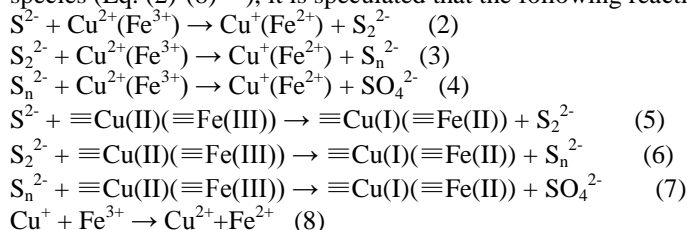


Fig. 3 XPS spectra of chalcopyrite: (a) Cu 2p before and after ozonation
(b) Fe 2p before and after ozonation

2.2 O 1s

In Fig. 4, three oxygen species were found on the surface of chalcopyrite: lattice oxygen (O^{2-}) at 530 eV, surface hydroxyl / sulfate ($\text{OH}/\text{SO}_4^{2-}$) at 531.1 eV and chemisorbed H_2O at 532.1 eV [27]. As can be seen, the percentage of lattice oxygen of chalcopyrite after participation in ozonation increased from 13.61% to 18.22%, indicating the generation of metal oxides during ozonation. The surface hydroxyl formed from the dissociation of water molecules coordinated with Fe^{2+} and Cu^{2+} on the surface of chalcopyrite decreased by 4.96% after ozonation, indicating that the surface hydroxyl groups of chalcopyrite were the active center and participated in the reaction to generate hydroxyl radicals.

Both the increase of the lattice oxygen and the decrease of the surface hydroxyl groups indicated that chalcopyrite played an important catalytic role in the catalytic ozonation system.

Finally the chemisorbed H₂O at 532.1 eV is slightly elevated, which is consistent with the analysis of S2p below that the oxidation of the chalcopyrite surface changes the sulfur fraction and thus the chalcopyrite surface became more hydrophilic than before.

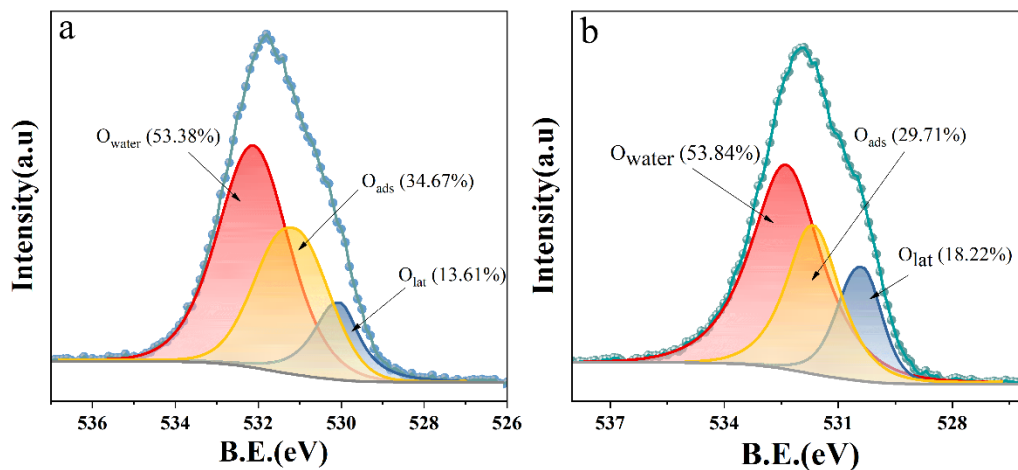


Fig. 4 XPS spectra of chalcopyrite: O 1s (a) before and (b) after ozonation

2.3 S 2p

The fitted S 2p spectra of chalcopyrite before and after ozonation are shown in Figure 5. The 2p_{3/2} fraction of S is located at 162.1 eV, which can be attributed to monosulfide S²⁻[11][14], and 2p_{3/2} peaks of disulfide S₂²⁻, polysulfide S_n²⁻, and sulfate SO₄²⁻ are located at 163.1 eV, 164.1 eV, and 169.0 eV, respectively^[30]. As can be seen, the proportions of the first three species (S²⁻, S₂²⁻, and S_n²⁻) decreased significantly after ozonation, while the proportion of sulfate increased significantly. On the one hand, it shows that sulfate formed from oxidation of chalcopyrite in this system was helpful to improve the hydrophilicity of minerals. On the other hand, the change of hydrophilicity makes it easier for O₃ in the liquid phase to contact the active sites on the chalcopyrite surface to produce free radicals such as •OH^[27].

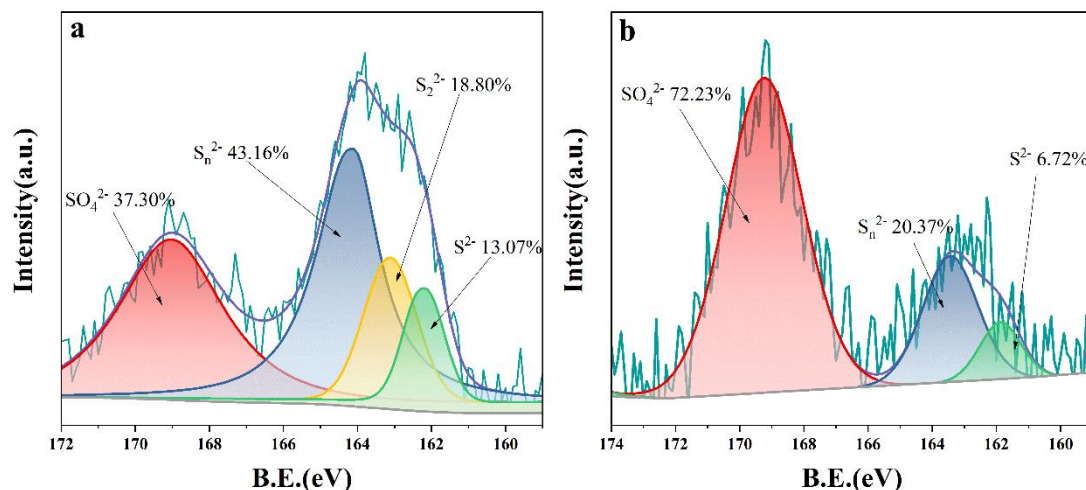


Fig. 5 XPS spectra of chalcopyrite: S 2p (a) before and (b) after ozonation

3. SEM

Fig.6 shows the surface morphology of chalcopyrite before and after catalytic ozonation observed by scanning electron microscope (SEM). It can be found that the surface of chalcopyrite was relatively smooth before the reaction and became rough after participating in the ozonation, many tiny particles were generated. Combined with the XPS characterization data, It could be concluded that the surface of chalcopyrite was partly oxidized after the reaction, and a certain amount of Fe and Cu oxides were formed. The study shows that the reaction between O₃ and chalcopyrite is a complex reaction, it includes two mechanisms of surface and solution reactions: direct oxidation and free radical oxidation^[10]. Direct oxidation means that O₃ is adsorbed to the Fe (II)

and Cu (I) sites on the surface of chalcopyrite^[13]. Free radical oxidation means that chalcopyrite is oxidized by the intermediate hydroxyl radicals of $\cdot\text{OH}$ produced during the reaction^[10].

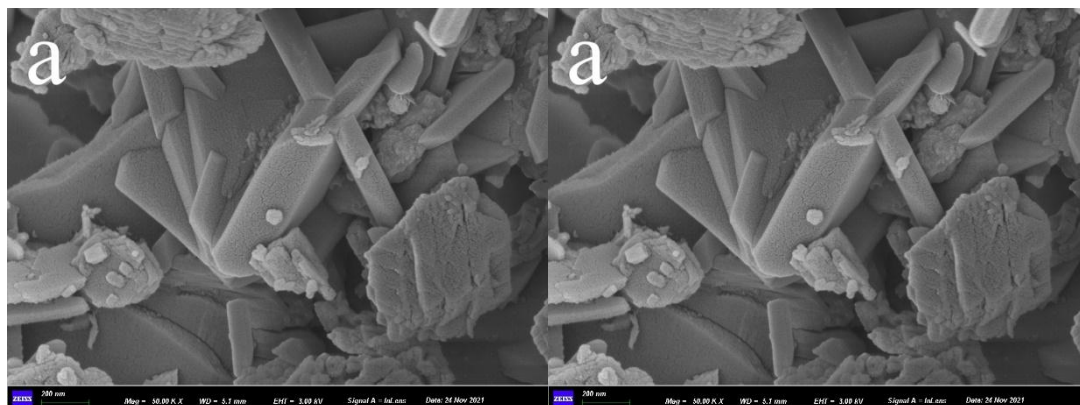


Fig. 6 SEM results of chalcopyrite (before and after catalytic ozonation before reaction, (d) after reaction

Catalytic performance of chalcopyrite

As Fig. 7 shows, under the conditions of initial pH value of 7.0, initial TOC concentration of 10mg/L, chalcopyrite dosage of 1g/L and aqueous ozone concentration of 8 mg/L, the effects of chalcopyrite adsorption, single ozonation and chalcopyrite/O₃ on the degradation efficiency of oxalic acid were studied. It can be seen that the system had no degradation effect on oxalic acid when only chalcopyrite was added to the simulated wastewater or ozone was introduced alone, indicating that: First. the adsorption of oxalic acid on chalcopyrite was small. Second. ozone had no degradation effect on oxalic acid. The removal percentage of oxalic acid by chalcopyrite/O₃ system was about 90%. This result showed that ozone produced a large number of active free radicals under the catalysis of chalcopyrite to attack oxalic acid to produce water and carbon dioxide.

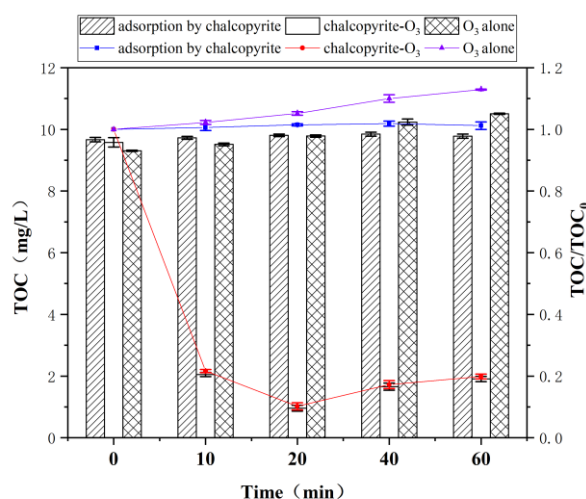


Fig. 7 Oxalic acid removal by chalcopyrite. (catalytic ozonation, adsorption and ozonation alone)

Effect of initial pH on catalytic ozonation

The effects of different initial pH values (5, 7 and 9) on the degradation efficiency of oxalic acid were analyzed by adjusting the solution pH under the conditions of the initial TOC 10 mg/L, chalcopyrite dosing of 0.2 g/L and aqueous ozone concentration of 8 mg/L.

Fig.8 (a) shows the removal of oxalic acid by catalytic ozonation of 15min with different initial pH values. In 5 min of reaction, the removal of oxalic acid under acidic condition (pH=5) was 70.2%, which was slightly different from that of 69.7% at pH 9, but when the initial pH in water was 7, the TOC removal increased to 91.3%. In order to get more intuitively understand the effect of the catalyst under different pH conditions, the first-order kinetic curve was fitted with the 5min removal efficiency. TOC is the concentration of carbon in

oxalic acid in the solution with time, and TOC_0 is the initial concentration of carbon in oxalic acid. Fig.8 (b) shows the change of $\ln(TOC/TOC_0)$ with time t . When pH is 7 and t is 5min, $\ln(TOC/TOC_0)$ is -2.46 and the slope k of the straight line under the pH is at the maximum of 0.50.

When the pH increased from acidic to alkaline conditions, ozone decomposition increased, leading to more production of $\cdot OH$ radicals. This indicates that solution pH had a strong influence on the catalytic ozonation process. Since the catalyst is negatively charged at higher pH, it generates repulsive electrostatic interaction between the contaminant and the catalyst, which reduces the surface reaction and thus leads to a decrease in oxalic acid removal efficiency. Protonation of $\cdot OH$ occurs when $pH < pH_{pzc}$, and deprotonation of $\cdot OH$ occurs when $pH > pH_{pzc}$. When the $pH_{pzc} = pH$, the hydroxyl group will be in a neutral state, which is conducive to the production of $\cdot OH$ radical and has a good catalytic effect. Therefore, there exists an optimal pH value for the catalytic ozonation system, which is close to the isoelectric point pH_{pzc} of the catalyst^[15].

The pH_{pzc} of chalcopyrite powder used in this experiment is 7.14. This is consistent with the experimental results that the removal of oxalic acid by catalytic ozonation at pH 7 has the highest TOC removal percentage and faster reaction rate (in 10 min).

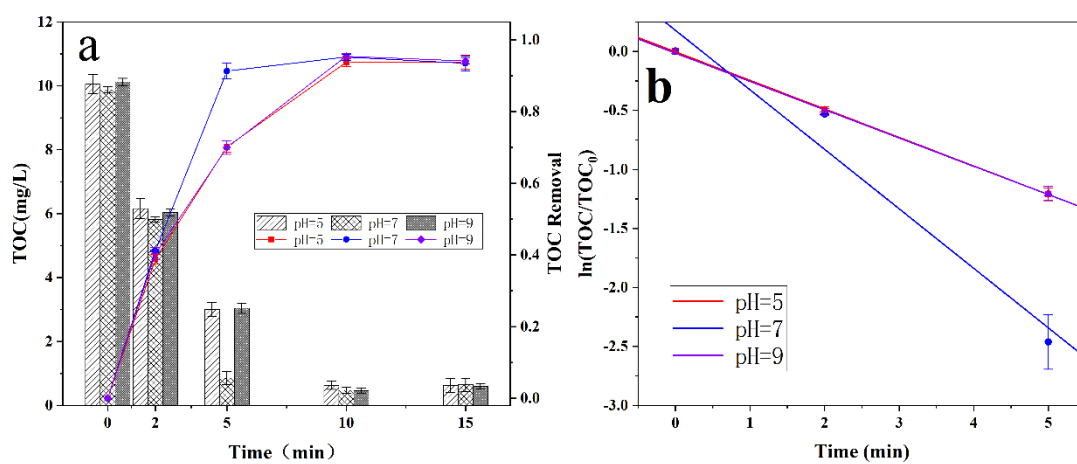


Fig. 8 The influence of different initial pH on the removal of oxalic acid by chalcopyrite catalyzed ozonation

Effect of ozone dosage on catalytic ozonation

Fig.9 (a) shows the degradation effect of chalcopyrite/ozone system for oxalic acid at different aqueous ozone dosage. The results showed that the difference of the degradation effect was especially obvious in the reaction time of 5 min at different aqueous ozone concentration. The degradation of oxalic acid was the lowest at 0.8 mg/L of aqueous ozone concentration, which was only 26.6%; it increased to 46.0% and 45.7% at 2 mg/L and 4 mg/L of aqueous ozone concentration, respectively; and the highest degradation percentage was 91.30% when the aqueous ozone concentration was 8 mg/L.

With the increase of ozone dosage, more ozone molecules were transported to the liquid phase and contacted with the catalyst surface to form $\cdot OH$ radicals. According to the first-order kinetic curve fitting within the first 5min, the corresponding first-order reaction rate constants of 0.8 mg/L, 2 mg/L, 4 mg/L and 8 mg/L aqueous ozone concentration were 0.063min^{-1} , 0.122min^{-1} , 0.125min^{-1} and 0.504min^{-1} , respectively. It can be seen that the degradation efficiency and reaction rate of oxalic acid in the catalytic ozonation system increased with the increase of ozone dosage.

For 8 mg/L aqueous ozone concentration, from 15 min, the effect of continuing to increase the ozone dosage on the degradation efficiency became small. Considering the cost of ozone, 8 mg/L would be the optimum ozone dosage for subsequent experiments.

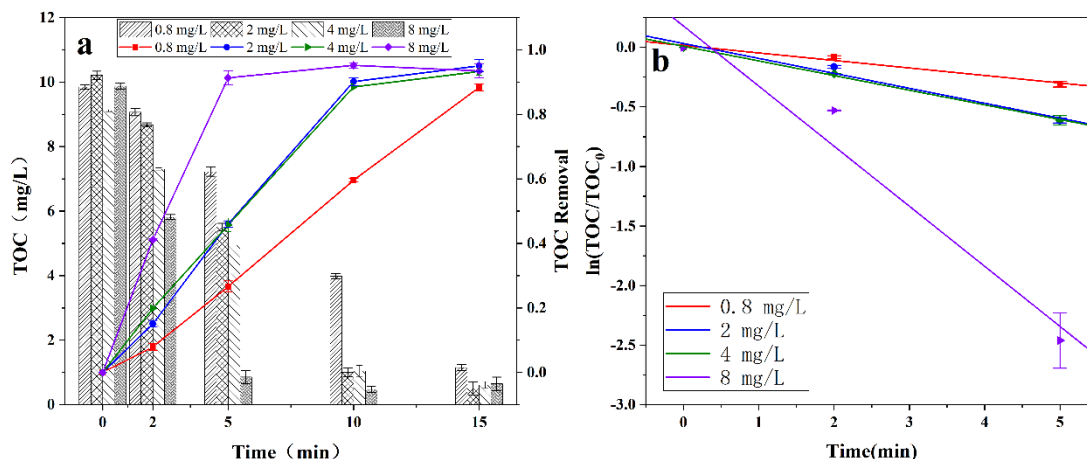


Fig. 9 The influence of different ozone dosage on the removal of oxalic acid by chalcopyrite catalyzed ozonation

Effect of catalyst dosage on catalytic ozonation

When catalytic ozonation proceeded for 5 min, From Fig.10(a), it is obvious that with the increase of catalyst dosage (0.05g/L, 0.1g/L, 0.2g/L, 0.6g/L, 1g/L), the effect of chalcopyrite in catalytic ozonation system improved. The corresponding oxalic acid degradation was 71.4%, 81.9% and 91.3% at the catalyst dosage of 0.05g/L, 0.1g/L and 0.2g/L. However, after continuing to increase the dosage to 3-5 times of 0.2g/L, the corresponding oxalic acid removal were 90.3% and 91.1%, respectively, thus the improvement of degradation efficiency became less obvious. At 15 min of reaction, the effect of different catalyst dosage tended to level off. The related studies showed that with the increase of catalyst dosage, on the one hand, chalcopyrite provided more specific surface area and active sites for ozone to generate more $\cdot\text{OH}$ radicals to achieve better effect. This can be easily seen from the First-order reaction kinetics fitting curves in Fig.10 (b), with the increase of catalyst dosage from 0.05 g/L, 0.1 g/L to 0.2 g/L, the corresponding first-order reaction rates were 0.257 min^{-1} , 0.351 min^{-1} and 0.472 min^{-1} , respectively, and the rate increase was obvious. On the other hand, excessive catalyst inhibits the collision between pollutants and $\cdot\text{OH}$ reactive radicals, which in turn affects the removal efficiency^[3]. The oxalic acid removal would not significantly increased by continuing to increase the catalyst dosage. In the process of actual industrial wastewater treatment, the cost of catalyst is also a factor to be considered, so the optimal dosage of catalyst was selected as 0.2 g/L for subsequent experiments.

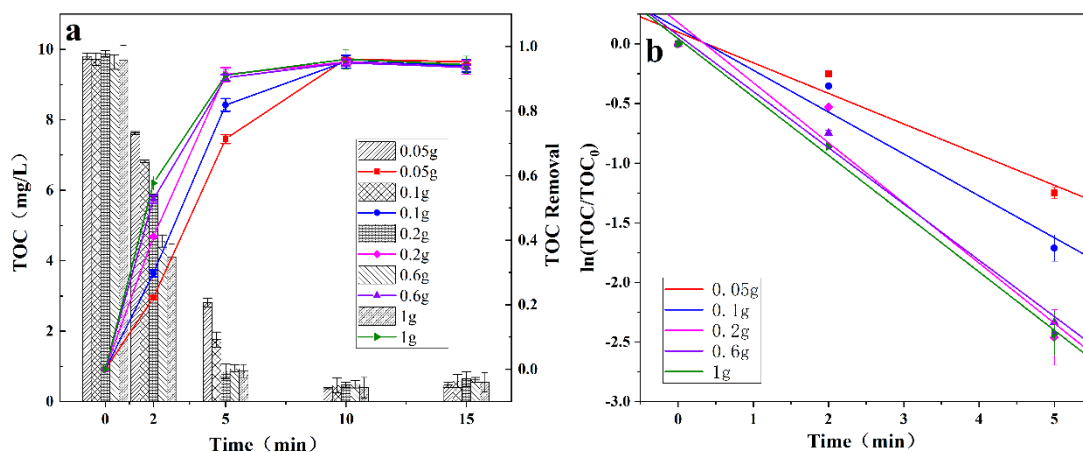


Fig. 10 The influence of catalyst dosage on the removal of oxalic acid by chalcopyrite catalyzed ozonation

Effect of initial oxalic acid concentration on catalytic ozonation

According to Fig. 11(a), when the initial oxalic acid concentration was increased from 5 mg/L to 10 mg/L TOC, the degradation was significantly improved by 10.7% in the reaction time of 10min. However, compared with 10 mg/L initial oxalic acid concentration, the degradation decreased by 18.4% (20 mg/L), 25.6% (30 mg/L) and 36.3% (40 mg/L), respectively. This might be because the specific surface area of the added catalyst was

limited, so the effective active sites provided for O₃ to generate •OH radical were also limited. Therefore, the pollutant removal was improved when the initial concentration increased from 5 mg/L to 10 mg/L. Continuing to increase the initial oxalic acid concentration would reveal that: on one hand, the active sites on the catalyst surface were saturated or even oversaturated; on the other hand, too many pollutants in the system would occupy most of the catalyst surface. The collision rate of O₃ on the surface of the catalyst was reduced, thus leading to a decrease in the number of active sites on its surface, which in turn led to a decrease in its final degradation efficiency. This could be easily seen from the first-order kinetic fitting curves in Fig. 11(b), where the first-order kinetic constants corresponding to initial oxalic acid concentrations of 20 mg/L, 30 mg/L, and 40 mg/L are 0.060 min⁻¹, 0.058 min⁻¹, and 0.045 min⁻¹, which are much less rapid than the 0.504 min⁻¹ corresponding to 10 mg/L. The removal efficiency at each concentration stabilized after the reaction was carried out for 15 min, although the removal rate decreased, the amount of TOC removed increased significantly from 9.35 mg/L to 33.54 mg/L. This might be due to the fact that the ozone was continuously increased within 15 min, which was oversaturated and sufficient, and the performance of the catalyst was excessive at the initial oxalic acid concentration of 10 mg/L, which was capable of degrading more pollutants; as the concentration of pollutants increased, the reaction rate decreased significantly

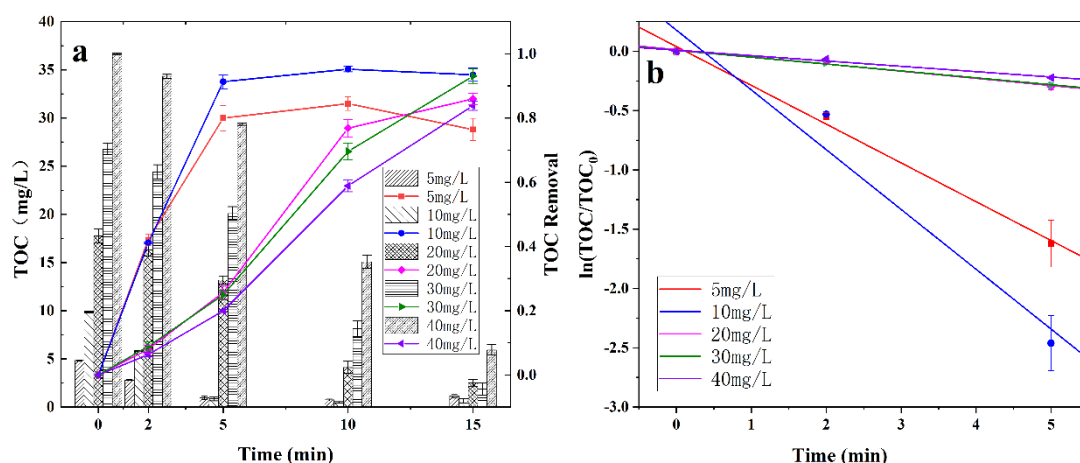
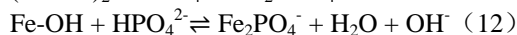
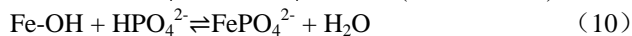
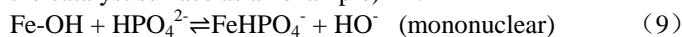


Fig. 11 The influence of initial oxalic acid concentration on the removal of oxalic acid by chalcopyrite catalyzed ozonation

IV. Possible Mechanism

It has been shown that phosphate exhibited a strong affinity to the catalyst surface, for phosphate adsorption was believed to occur through ligand exchange accompanied by phosphate deprotonation, whether phosphate replaces one or two hydroxyl groups on the catalyst surface (i.e., forming a mononuclear or binuclear bond) is still a matter of debate. It is speculated that the substitution of surface hydroxyl groups had an effect on the catalytic performance of chalcopyrite, and the following reactions might take place. (Eq.(9)-(12) using Fe on the catalyst surface as an example) [19].



As can be seen from Fig.12, after adding 0.002 mol/L and 0.005 mol/L K₂HPO₄ to the catalytic ozonation system with the initial oxalic acid concentration of 10 mg/L (TOC), initial pH=7, ozone flow rate and catalyst dosage of 2 L/min and 0.2 g/L, respectively, it can be clearly seen that the oxalic acid removal decreased from 93.5% to 44.8% and 24.4%, the reaction rates also slowed down, and the working efficiency of the catalysts decreased sharply.

This once again shows the importance of active sites on the catalyst, where phosphate occupied the active center of the catalyst surface, cut off the pathway of O₃ molecules to form hydroxyl radicals and made the catalyst less effective. In addition, under the addition of 0.006 mol/L and 0.010 mol/L carbonate to the system, the oxalic acid removal decreased slightly by 3.1% and 5.5%, which might be related to the reaction of bicarbonate ions with •OH radicals as shown in Fig.(13) and (14). At the same time, CO₃^{•-} radicals with lower oxidation potential than •OH and higher selectivity were formed [5]. It can be seen that carbonate, as an inhibitor, mainly reacted with •OH radicals in solution, whereas did not affect the way of forming hydroxyl radicals on the catalyst surface. Moreover, the aqueous ozone concentration in this experiment was saturated, so carbonate

had some influence on the pollutant removal efficiency in this catalytic ozonation system, but the effect was not significant.

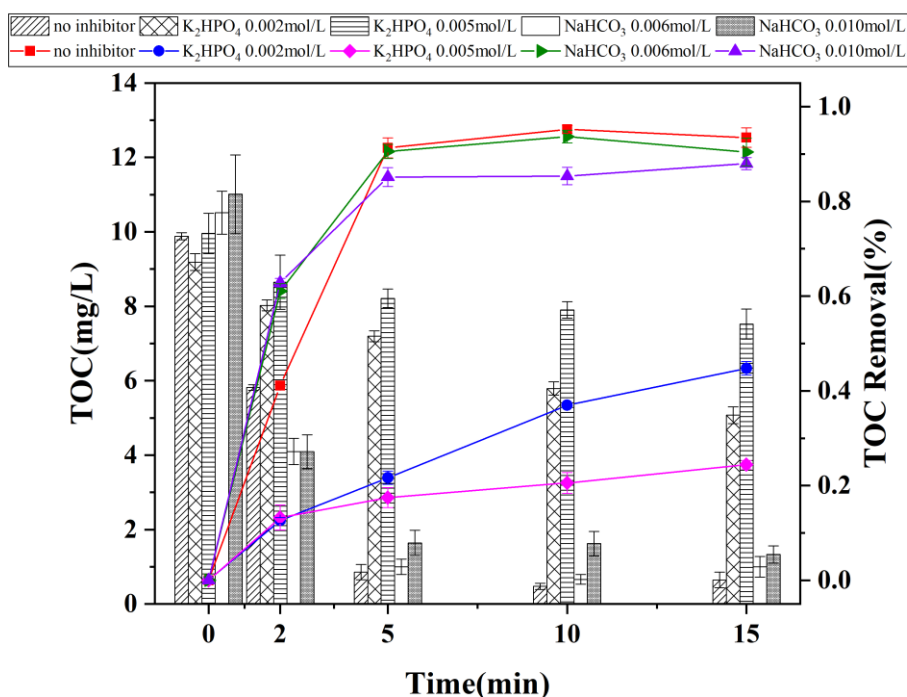
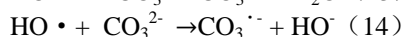
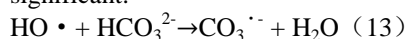


Fig.12 The effect of phosphate and carbonate on catalytic ozonation of oxalic acid

The following Fig.13 presents the interfacial reaction mechanism of chalcopyrite catalyzed ozonation. First, O_3 dissolved in liquid phase contacted the chalcopyrite surface, then combined with Me-OH (Me: Cu, Fe) groups to initiate a series of free radical reactions at active center, and free active substances such as $\cdot\text{OH}$ and $\cdot\text{O}_2^-$ were generated consequently. On the catalyst surface, S^{2-} , S_2^{2-} and S_n^{2-} as electron donors played a key role in participating in and promoting the recycling of $\text{Fe}^{3+}/\text{Fe}^{2+}$ and $\text{Cu}^{2+}/\text{Cu}^+$ in the chalcopyrite / O_3 system, and the electron transfer between polymetals in this cycle could further promote the decomposition of O_3 to produce more free radicals^[23]. Second, the sulfur species S^{2-} , S_2^{2-} , S_n^{2-} would produce SO_4^{2-} during the cycle. Studies have shown that $\cdot\text{OH}$ free radicals could react with them to form $\text{SO}_4^{\cdot -}$ ^[6]. Finally, these free radicals attacked oxalic acid to produce water and carbon dioxide, which was finally mineralized.

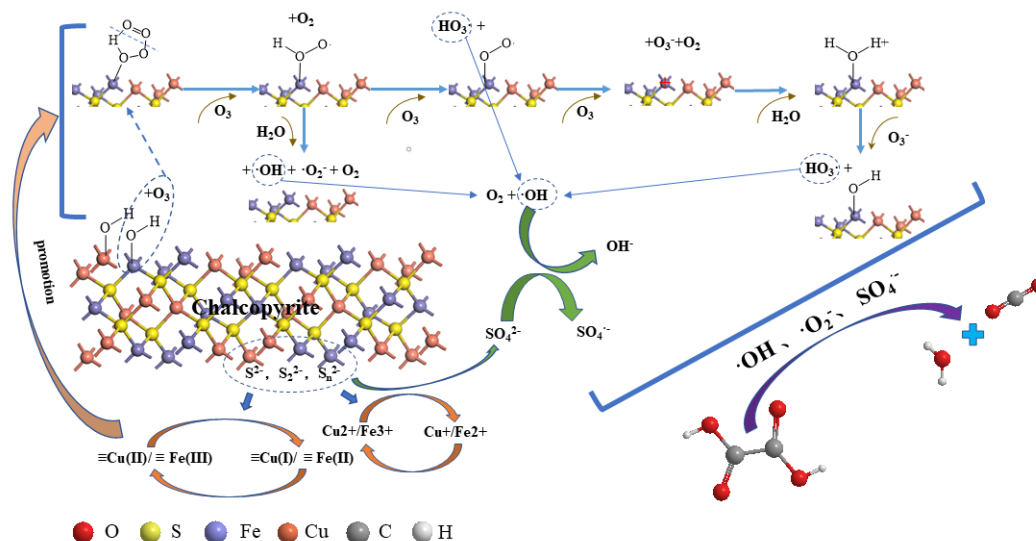


Fig. 13 The mechanism of chalcopyrite catalyzed ozonation to degrade oxalic acid

V. Conclusion

In this study, it was found that natural chalcopyrite have a good catalytic performance in ozonation for the removal of oxalic acid. The effect of pH, ozone dosage, chalcopyrite dosage and initial concentration of oxalic acid on oxalic acid removal were studied. When the solution pH was close to the pH_{pzc} of chalcopyrite, the degradation of oxalic acid was the highest; higher ozone dosage led to the production of more active oxygen and higher oxalic acid removal; considering the economic cost of the catalyst, the optimal chalcopyrite dosage and initial concentration of pollutants in the system were determined. It was concluded that chalcopyrite stimulated the production of some free radicals like $\cdot\text{OH}$, $\cdot\text{O}^{2-}$ and $\text{SO}_4^{\cdot-}$ to attack pollutants and achieved the purpose of mineralization. The natural chalcopyrite selected in this research has the characteristics of low cost, easy to obtain and high reactivity, and has good practical application value in the treatment of organic pollutant wastewater.

Acknowledgment

This research was supported by the National Natural Science Foundation of China (No. 21876111).

REFERENCES

- [1]. Dong, C., W. Fang, Q. Yi and J. Zhang (2022). "A comprehensive review on reactive oxygen species (ROS) in advanced oxidation processes (AOPs)." *Chemosphere* 308(Pt 1): 136205. <http://dx.doi.org/10.1016/j.chemosphere.2022.136205>
- [2]. Droguett, C., R. Salazar, E. Brillas, I. Sires, C. Carlesi, J. F. Marco and A. Thiam (2020). "Treatment of antibiotic cephalexin by heterogeneous electrochemical Fenton-based processes using chalcopyrite as sustainable catalyst." *Sci Total Environ* 740: 140154. <http://dx.doi.org/10.1016/j.scitotenv.2020.140154>
- [3]. Faghihinezhad, M., M. Baghdadi, M. S. Shahin and A. Torabian (2022). "Catalytic ozonation of real textile wastewater by magnetic oxidized g-C₃N₄ modified with Al₂O₃ nanoparticles as a novel catalyst." *Separation and Purification Technology* 283. <http://dx.doi.org/10.1016/j.seppur.2021.120208>
- [4]. Faria, P. C. C., J. J. M. Orfão and M. F. R. Pereira (2008). "Activated carbon catalytic ozonation of oxamic and oxalic acids." *Applied Catalysis B: Environmental* 79(3): 237-243. <http://dx.doi.org/10.1016/j.apcatb.2007.10.021>
- [5]. Ghuge, S. P. and A. K. Saroha (2018). "Catalytic ozonation of dye industry effluent using mesoporous bimetallic Ru-Cu/SBA-15 catalyst." *Process Safety and Environmental Protection* 118: 125-132. <http://dx.doi.org/10.1016/j.psep.2018.06.033>
- [6]. Hara, J. (2017). "Oxidative degradation of benzene rings using iron sulfide activated by hydrogen peroxide/ozone." *Chemosphere* 189: 382-389. <http://dx.doi.org/10.1016/j.chemosphere.2017.09.081>
- [7]. Huang, G.-Y., W.-J. Chang, T.-W. Lu, I. L. Tsai, S.-J. Wu, M.-H. Ho and F.-L. Mi (2022). "Electrospun CuS nanoparticles/chitosan nanofiber composites for visible and near-infrared light-driven catalytic degradation of antibiotic pollutants." *Chemical Engineering Journal* 431. <http://dx.doi.org/10.1016/j.cej.2021.134059>
- [8]. Huang, X., T. Zhu, W. Duan, S. Liang, G. Li and W. Xiao (2020). "Comparative studies on catalytic mechanisms for natural chalcopyrite-induced Fenton oxidation: Effect of chalcopyrite type." *J Hazard Mater* 381: 120998. <http://dx.doi.org/10.1016/j.jhazmat.2019.120998>
- [9]. Huang, Y., Y. Sun, Z. Xu, M. Luo, C. Zhu and L. Li (2017). "Removal of aqueous oxalic acid by heterogeneous catalytic ozonation with MnO(x)/sewage sludge-derived activated carbon as catalysts." *Sci Total Environ* 575: 50-57. <http://dx.doi.org/10.1016/j.scitotenv.2016.10.026>
- [10]. Lefticariu, L., A. Schimmelmann, L. M. Pratt and E. M. Ripley (2007). "Oxygen isotope partitioning during oxidation of pyrite by H₂O₂ and its dependence on temperature." *Geochimica et Cosmochimica Acta* 71(21): 5072-5088. <http://dx.doi.org/10.1016/j.gca.2007.08.022>
- [11]. Li, Y., A. P. Chandra and A. R. Gerson (2014). "Scanning photoelectron microscopy studies of freshly fractured chalcopyrite exposed to O₂ and H₂O." *Geochimica et Cosmochimica Acta* 133: 372-386. <http://dx.doi.org/10.1016/j.gca.2014.02.037>
- [12]. Liu, J., J. Li, S. He, L. Sun, X. Yuan and D. Xia (2020). "Heterogeneous catalytic ozonation of oxalic acid with an effective catalyst based on copper oxide modified g-C₃N₄." *Separation and Purification Technology* 234. <http://dx.doi.org/10.1016/j.seppur.2019.116120>
- [13]. McKibben, M. A. and H. L. Barnes (1986). "Oxidation of pyrite in low temperature acidic solutions: Rate laws and surface textures." *Geochimica et Cosmochimica Acta* 50(7): 1509-1520. [http://dx.doi.org/https://doi.org/10.1016/0016-7037\(86\)90325-X](http://dx.doi.org/https://doi.org/10.1016/0016-7037(86)90325-X)
- [14]. Moimane, T., C. Plackowski and Y. Peng (2020). "The critical degree of mineral surface oxidation in copper sulphide flotation." *Minerals Engineering* 145. <http://dx.doi.org/10.1016/j.mineng.2019.106075>
- [15]. Munir, H. M. S., N. Feroze, N. Ramzan, M. Sagir, M. Babar, M. S. Tahir, J. Shamshad, M. Mubashir and K. S. Khoo (2022). "Fe-zeolite catalyst for ozonation of pulp and paper wastewater for sustainable water resources." *Chemosphere* 297: 134031. <http://dx.doi.org/10.1016/j.chemosphere.2022.134031>
- [16]. Panda, S., A. Akcil, N. Pradhan and H. Deveci (2015). "Current scenario of chalcopyrite bioleaching: a review on the recent advances to its heap-leach technology." *Bioresour Technol* 196: 694-706. <http://dx.doi.org/10.1016/j.biortech.2015.08.064>
- [17]. Pei, L. Z., J. F. Wang, X. X. Tao, S. B. Wang, Y. P. Dong, C. G. Fan and Q.-F. Zhang (2011). "Synthesis of CuS and Cu_{1.1}Fe_{1.1}S₂ crystals and their electrochemical properties." *Materials Characterization* 62(3): 354-359. <http://dx.doi.org/10.1016/j.matchar.2011.01.001>
- [18]. Peng, J., H. Zhou, W. Liu, Z. Ao, H. Ji, Y. Liu, S. Su, G. Yao and B. Lai (2020). "Insights into heterogeneous catalytic activation of peroxymonosulfate by natural chalcopyrite: pH-dependent radical generation, degradation pathway and mechanism." *Chemical Engineering Journal* 397. <http://dx.doi.org/10.1016/j.cej.2020.125387>
- [19]. Sui, M., L. Sheng, K. Lu and F. Tian (2010). "FeOOH catalytic ozonation of oxalic acid and the effect of phosphate binding on its catalytic activity." *Applied Catalysis B: Environmental* 96(1-2): 94-100. <http://dx.doi.org/10.1016/j.apcatb.2010.02.005>
- [20]. Sun, Y., M. Danish, M. Ali, A. Shan, M. Li, Y. Lyu, Z. Qiu, Q. Sui, X. Zang and S. Lyu (2020). "Trichloroethene degradation by nanoscale CaO₂ activated with Fe(II)/FeS: The role of FeS and the synergistic activation mechanism of Fe(II)/FeS." *Chemical Engineering Journal* 394. <http://dx.doi.org/10.1016/j.cej.2020.124830>
- [21]. Wang, B., H. Zhang, F. Wang, X. Xiong, K. Tian, Y. Sun and T. Yu (2019). "Application of Heterogeneous Catalytic Ozonation for Refractory Organics in Wastewater." *Catalysts* 9(3). <http://dx.doi.org/10.3390/catal9030241>

- [22]. Wang, H., B. Liao, M. Hu, Y. Ai, L. Wen, S. Yang, Z. Ye, J. Qin and G. Liu (2022). "Heterogeneous activation of peroxymonosulfate by natural chalcopyrite for efficient remediation of groundwater polluted by aged landfill leachate." *Applied Catalysis B: Environmental* 300. <http://dx.doi.org/10.1016/j.apcatb.2021.120744>
- [23]. Wang, J. and H. Chen (2020). "Catalytic ozonation for water and wastewater treatment: Recent advances and perspective." *Sci Total Environ* 704: 135249. <http://dx.doi.org/10.1016/j.scitotenv.2019.135249>
- [24]. Wang, J. L. and L. J. Xu (2012). "Advanced Oxidation Processes for Wastewater Treatment: Formation of Hydroxyl Radical and Application." *Critical Reviews in Environmental Science and Technology* 42(3): 251-325. <http://dx.doi.org/10.1080/10643389.2010.507698>
- [25]. Xia, J.-l., J.-j. Song, H.-c. Liu, Z.-y. Nie, L. Shen, P. Yuan, C.-y. Ma, L. Zheng and Y.-d. Zhao (2018). "Study on catalytic mechanism of silver ions in bioleaching of chalcopyrite by SR-XRD and XANES." *Hydrometallurgy* 180: 26-35. <http://dx.doi.org/10.1016/j.hydromet.2018.07.008>
- [26]. Xie, Y., S. Peng, Y. Feng and D. Wu (2020). "Enhanced mineralization of oxalate by highly active and Stable Ce(III)-Doped g-C(3)N(4) catalyzed ozonation." *Chemosphere* 239: 124612. <http://dx.doi.org/10.1016/j.chemosphere.2019.124612>
- [27]. Yang, X., Y. Li, R. Fan, W. Duan, L. Huang and Q. Xiao (2022). "Separation mechanism of chalcopyrite and pyrite due to H₂O₂ treatment in low-alkaline seawater flotation system." *Minerals Engineering* 176. <http://dx.doi.org/10.1016/j.mineng.2021.107356>
- [28]. Yin, H., J. Liu, H. Shi, L. Sun, X. Yuan and D. Xia (2022). "Highly efficient catalytic ozonation for oxalic acid mineralization with Ag₂CO₃ modified g-C₃N₄: Performance and mechanism." *Process Safety and Environmental Protection* 162: 944-954. <http://dx.doi.org/10.1016/j.psep.2022.04.060>
- [29]. Zhang, H., F. Zhang, W. Sun, D. Chen, J. Chen, R. Wang, M. Han and C. Zhang (2023). "The effects of hydroxyl on selective separation of chalcopyrite from pyrite: A mechanism study." *Applied Surface Science* 608. <http://dx.doi.org/10.1016/j.apsusc.2022.154963>
- [30]. Zhao, C., B. Yang, R. Liao, M. Hong, S. Yu, J. Wang and G. Qiu (2022). "Catalytic mechanism of manganese ions and visible light on chalcopyrite bioleaching in the presence of Acidithiobacillusferrooxidans." *Chinese Journal of Chemical Engineering* 41: 457-465. <http://dx.doi.org/10.1016/j.cjche.2021.10.009>
- [31]. Zhao, H., X. Huang, J. Wang, Y. Li, R. Liao, X. Wang, X. Qiu, Y. Xiong, W. Qin and G. Qiu (2017). "Comparison of bioleaching and dissolution process of p-type and n-type chalcopyrite." *Minerals Engineering* 109: 153-161. <http://dx.doi.org/10.1016/j.mineng.2017.03.013>
- [32]. Zhou, X., Z. Luo, P. Tao, B. Jin, Z. Wu and Y. Huang (2014). "Facile preparation and enhanced photocatalytic H₂-production activity of Cu(OH)₂ nanospheres modified porous g-C₃N₄." *Materials Chemistry and Physics* 143(3): 1462-1468. <http://dx.doi.org/10.1016/j.matchemphys.2013.11.066>